ELSEVIER

Mechanisms of Development 102 (2001) 33–44

www.elsevier.com/locate/modo

Mice with a homozygous gene trap vector insertion in *mgcRacGAP* die during pre-implantation development

Tom Van de Putte[a], An Zwijsen[a], Olivier Lonnoy[a], Vladimir Rybin[b], Miranda Cozijnsen[a], Annick Francis[a], Veerle Baekelandt[c], Christine A. Kozak[d], Marino Zerial[b], Danny Huylebroeck[a,*]

[a]*Department of Cell Growth, Differentiation and Development (VIB-07), Flanders Interuniversity Institute for Biotechnology (VIB) and Laboratory of Molecular Biology (CELGEN), University of Leuven, Herestraat 49, 3000 Leuven, Belgium*
[b]*Max Planck Institute for Molecular Cell Biology and Genetics, Dresden, Germany*
[c]*Laboratory for Experimental Neurosurgery and Neuroanatomy, University of Leuven, Leuven, Belgium*
[d]*Laboratory of Molecular Microbiology, National Institute of Allergy and Infectious Diseases, National Institutes of Health, Bethesda, MD, USA*

Received 21 November 2000; received in revised form 22 December 2000; accepted 22 December 2000

Abstract

In a phenotypic screen in mice using a gene trap approach in embryonic stem cells, we have identified a recessive loss-of-function mutation in the *mgcRacGAP* gene. Maternal protein is present in the oocyte, and *mgcRacGAP* gene transcription starts at the four-cell stage and persists throughout mouse pre-implantation development. Total *mgcRacGAP* deficiency results in pre-implantation lethality. Such E3.5 embryos display a dramatic reduction in cell number, but undergo compaction and form a blastocoel. At E3.0–3.5, binucleated blastomeres in which the nuclei are partially interconnected are frequently observed, suggesting that mgcRacGAP is required for normal mitosis and cytokinesis in the pre-implantation embryo. All homozygous mutant blastocysts fail to grow out on fibronectin-coated substrates, but a fraction of them can still induce decidual swelling in vivo. The *mgcRacGAP* mRNA expression pattern in post-implantation embryos and adult mouse brain suggests a role in neuronal cells. Our results indicate that mgcRacGAP is essential for the earliest stages of mouse embryogenesis, and add evidence that CYK-4-like proteins also play a role in microtubule-dependent steps in the cytokinesis of vertebrate cells. In addition, the severe phenotype of *null* embryos indicates that mgcRacGAP is functionally non-redundant and cannot be substituted by other GAPs during early cleavage of the mammalian embryo.

Keywords: Blastocyst; Cytokinesis; Gene trapping; Pre-implantation development; GTPase-activating protein

1. Introduction

Gene trapping is an approach for random insertion mutagenesis in cultured cells which uses a vector DNA coding for a reporter and/or a dominant selectable marker gene as mutagen. One class of promoter-less gene trap vectors, which contains a splice acceptor site preceding the reporter gene, is designed such that the intracellular reporter protein is only synthesized when the vector integrates into an intron of an actively transcribed gene. Occasionally, integration of the vector in an exon might also result in a functional gene trap event, if spliced to the preceding splice donor. The vector serves as a tag enabling the identification and cloning of the mutated gene or cDNA and, subsequently, the wild-type counterparts. When applied to murine embryonic stem (ES) cells, gene trapping couples gene discovery to a loss-of-function approach in the mouse (Joyner et al., 1992). In addition, there is a high probability that the location of the reporter protein in the mouse embryo will reflect the expression pattern of the endogenous gene (Gossler et al., 1989).

Nuclear division during mitosis requires the activation of a cascade of events that tightly controls the duplication of the genetic information of the parental cell and the accurate segregation of the sister chromatids normally followed by cytokinesis, ultimately producing two daughter nuclei. The latter two fundamental processes appear to rely highly on tubulin-based mitotic spindles. These are, respectively, the astral mitotic spindles which are responsible for accurate chromosome segregation during mitosis, and the midzone central spindle which forms during anaphase and, in animal cells, determines the position of the actomyosin-based cleavage furrow and is required for the completion of cytokin-

* Corresponding author. Tel.: +32-16-345916; fax: +32-16-345933.
E-mail address: danny.huylebroeck@med.kuleuven.ac.be (D. Huylebroeck).

0925-4773/01/$ - see front matter
PII: S0925-4773(01)00279-9

esis. A dynamic interaction between the microtubule-based mitotic spindles and the actin filaments is therefore crucial. Tubulin-based mitotic motors have a major impact on cortical movements and actin filament redistribution during cell division. Reversibly, the cell cortex generates part of the mitotic forces (Fishkind et al., 1996). Therefore, aberrant functioning of the microtubuli may lead to aneuploidy, cancer and cell death.

RhoGTPases are key players in cell adhesion, motility, cytokinesis and contractile responses because of their involvement in growth factor-induced assembly and reorganization of the actin cytoskeleton (Hall, 1994). In addition, they are important in vesicle transport, secretion, phagocytosis and organelle motility (Murphy et al., 1996; Narumiya, 1996; Van Aelst and D'Souza-Schorey, 1997; Nobes and Hall, 1999). Along with these pleiotropic functions, Rho-like GTPases participate in the regulation of signalling to the nucleus, i.e. the transcriptional response (Hill et al., 1995), and in cell cycle control (Olson et al., 1995). RhoGTPases, represented by the intensively studied Rho, Rac and the cell division cycle 42 (Cdc42) proteins, act as binary molecular switches. Their activity is determined by the ratio of GTP-bound (active) versus GDP-bound (inactive) configurations. The nucleotide occupancy is regulated by the opposing effects of guanine nucleotide exchange factors (GEFs) that enhance the exchange of bound GDP by GTP, and by the downregulating effect of GTPase-activating proteins (GAPs) that increase the hydrolysis of the bound GTP (Boguski and McCormick, 1993; Van Aelst and D'Souza-Schorey, 1997).

Here, we report that vector-mediated gene disruption in ES cells has abolished the GAP, mgcRacGAP (Wooltorton et al., 1999; Arar et al., 1999; Kawashima et al., 2000). Perhaps because the RhoGAPs are involved in a multitude of basic cell functions, and redundancy is expected amongst the more than 15 members identified to date (Van Aelst and D'Souza-Schorey, 1997), gene targeting studies in the mouse with the aim of documenting their in vivo role have been rare (Voncken et al., 1995). In the study presented here, an essential GAP gene was identified in a phenotypic screen in mice, using a gene trap approach in ES cells. Deprivation of mgcRacGAP protein in homozygous mutant mouse embryos results in the formation of multinucleated blastomeres with interconnected nuclei as the embryos continue to cycle through mitosis but fail to complete cytokinesis, leading to pre-implantation lethality.

2. Results

2.1. Cloning of the fusion gtl11/βgeo and wild-type cDNA

The *gene trap locus 11* (*gtl11*) mutant allele was isolated in a gene trap screen for genes essential for embryonic development. In the case of *gtl11*, the heterozygous mutant ES cell clone was obtained by stable transformation of RW4 cells with pSAβgeo (Friedrich and Soriano, 1991). Southern blot analysis with the lacZ open reading frame as a probe showed that this ES cell line possesses a single pSAβgeo integration in the genome (data not shown). Chimeric mice were made by the aggregation of *gtl11* ES cells to morulae (Wood et al., 1993), and germ-line transmission of the mutated allele was obtained. *Gtl11* ES cells (data not shown) and heterozygous embryos produce β-galactosidase (βgal).

The mutant allele-encoded *gtl11/βgeo* hybrid mRNA was isolated as partial cDNA by 5′-RACE, starting from total RNA of *gtl11* ES cells. Analysis of the 144 bp-long RACE product indicated proper splicing between an exon from the trapped endogenous gene and the Adenoviral splice acceptor site of pSAβgeo. Sequences of overlapping cDNAs isolated from libraries, of EST clones and 5′-RACE products (data not shown) were subsequently used to assemble the wild-type mRNA sequence (accession numbers, AF212320 and AF212321). The encoded protein with a predicted size of 70.2 kDa appeared identical to the putative product encoded by 'band 25', which was originally identified in terminally differentiating 3T3-L1 adipocytes (Wooltorton et al., 1999) and was renamed mgcRacGAP (Touré et al., 1998; Arar et al., 1999; Kawashima et al., 2000). In agreement with others, we isolated two transcripts differing in their 3′-untranslated region (3′-UTR) by 775 bp due to alternative polyadenylation usage (here referred to as variants A and B). Significant similarity (91%; data not shown) was found with human MgcRacGAP (Touré et al., 1998; Kawashima et al., 2000). In vitro human MgcRacGAP catalyses the GTP hydrolysis of the Rho-like GTPases, Rac1 and Cdc42 (Touré et al., 1998; Kawashima et al., 2000). In addition, mgcRacGAP protein was found to be highly related (38% similarity; data not shown) to the recently characterized *C. elegans* protein CYK-4 (Jantsch-Plunger et al., 2000) and a *Drosophila* putative protein (46% similarity; accession number, CG13345; data not shown). All these proteins have a similar overall structure: the C-terminal half of the protein contains the typical catalytic part of GAPs that are specific for the Rho/Rac subgroup of small GTPases (Lamarche and Hall, 1994). This GAP^{Rho} domain is preceded by a C_6H_2 zinc-binding domain and the N-terminal half of the protein has evolutionary conserved hydrophobic features with an ultimate N-terminal segment that is likely to adopt a coiled-coil structure.

The mouse gene localizes at the distal end of chromosome15, distal to *Wnt-1* (data not shown). This region in the mouse is homologous to 12q13 in humans, as was confirmed by the mapping of a homologous human EST sequence (U82984; Volorio et al., 1998).

2.2. Expression of mgcRacGAP in vivo

The expression of *gtl11/βgeo* mRNA was monitored using βgal detection in heterozygous $mgcRacGAP^{gtl11/\beta geo}$ mouse embryos, and in situ hybridization with a *mgcRac-*

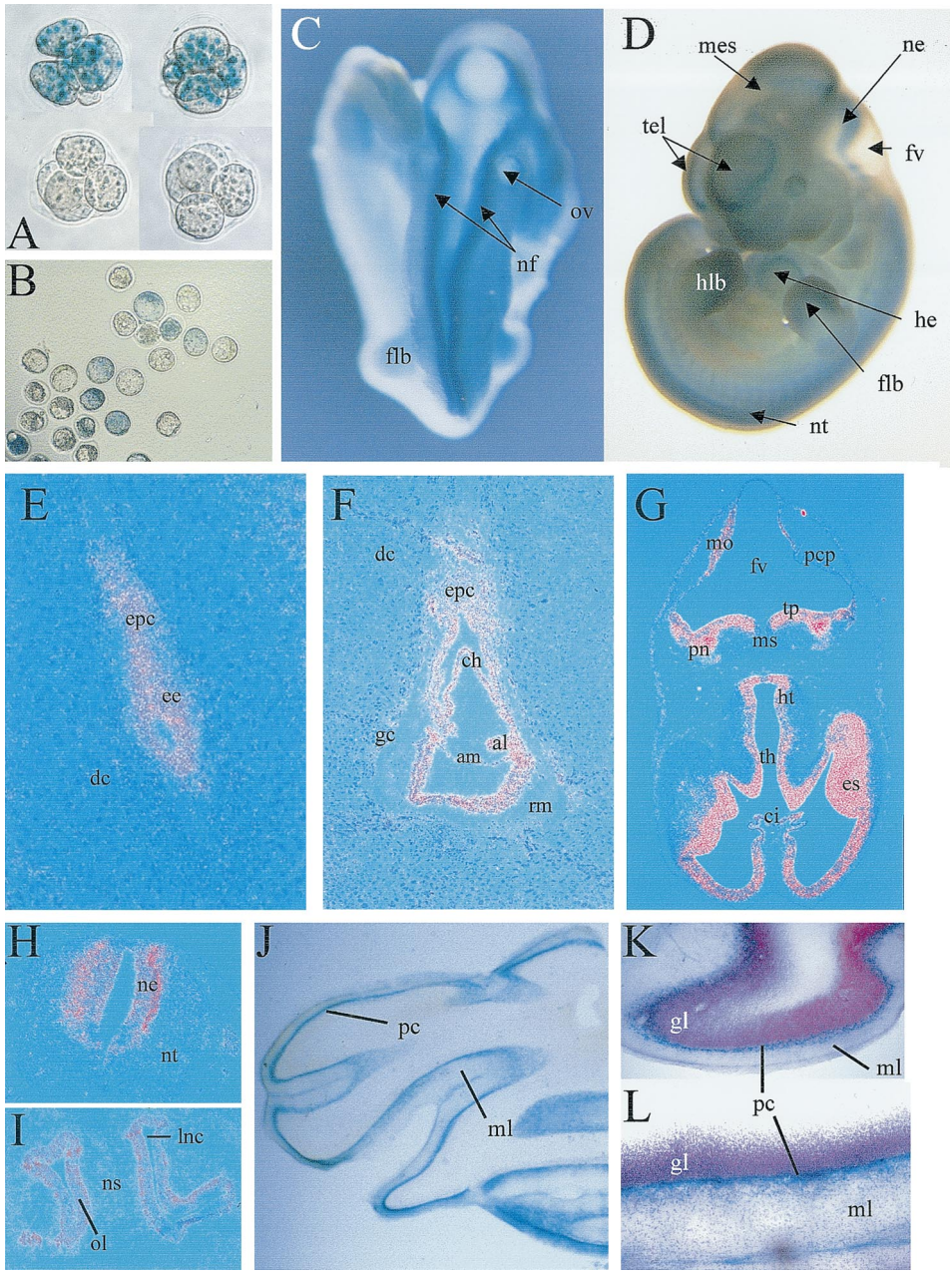

Fig. 1. Expression of *mgcRacGAP* in the mouse embryo and in adult brain. (A,B) Staining of pre-implantation embryos (from wild-type female × heterozygous male crosses) with X-gal: (A), four-cell stage (E1.5); and (B), blastocyst-stage (E3.5) embryos. (C,D) Brief whole-mount X-gal staining of heterozygous *gtl11* embryos. (C) E9.5 embryos (dorsal view) stain strongly in the neural folds. (D) At E12.5, reporter levels are elevated in the neural epithelium of the neural tube and the brain vesicles, and to a lesser extent in the limb buds and the heart. (E–I) In situ hybridization of mgcRacGAP mRNA in wild-type embryos. Sagittal sections of: (E), E6.5; and (F), E7.5 embryos within the deciduum; (G), transverse section of an E12.5 embryo at the level of the head; (H), further magnifications of the neural tube at E12.5; (I), magnification of the nasal region at E12.5; (J), localization of βgal activity in the cerebellum of adult heterozygous mice. (K,L) magnifications of adult heterozygous *p70GAP*$^{gtl11/\beta geo}$ cerebellum stained with X-gal. The Purkinje cell layer stains positive and βgal producing cells extend into the molecular layer. The granular layer, counterstained with Cresyl Violet, is devoid of βgal positive cells. al, Allantois; am, amnion; ch, chorion; dc, deciduum; ci, choroid invagination; ee, embryonic ectoderm; epc, ectoplacental cone; es, epithelial sulcus; flb, forelimb bud; fv, fourth ventricle; gc, giant cells; gl, granular layer; he, heart; hlb, hindlimb buds; ht, hypothalamus; lnc, lumen of the primitive nasal cavity; mes, mesencephalon; ml, molecular layer; mo, medula oblongata; ms, median sulcus; ne, neural epithelium; nf, neural fold; ns, nasal septum; nt, neural tube; ol, olfactory epithelium; ov, otic vesicle; pc, Purkinje cells; pcp, posterior choroid plexus; pn, pontine nucleus primordium; rm, Reichert's membrane; tel, cerebral hemisphere; th, thalamus; tp, tegmentum of the pons.

GAP riboprobe in wild-type embryos. Transcription of the trapped allele was assessed in zygotic embryos obtained from crosses between wild-type females and heterozygous males. Positive staining for βgal was detected from the four-cell stage (E2.0; Fig. 1A). It persisted in morulae (E2.5; data not shown), and was present both in the inner cell mass and

trophectoderm of blastocysts (Fig. 1B). Embryos resulting from an inverse cross showed βgal activity in fertilized oocytes (data not shown).

In situ hybridization on sections of mouse embryos at different stages of post-implantation development (Fig. 1E–I) was carried out using an antisense RNA probe of *mgcRacGAP*. No significant signals were detected using the sense probe (data not shown). *MgcRacGAP* was expressed at all stages analyzed (E6.5–12.5). At E6.5 (Fig.1E), primitive endoderm, embryonic ectoderm, extra-embryonic ectoderm and its derivative, the ectoplacental cone, were positive. The decidual tissue surrounding the embryo was devoid of *mgcRacGAP* mRNA. At E7.5 (advanced primitive streak stage; Fig. 1F), a widespread expression pattern was observed in all intra- and extra-embryonic tissues. The giant cells lining the inner boundary of the deciduum express *mgcRacGAP* also. At E8.5, the mRNA persisted in the embryo proper, all extra-embryonic membranes, and in trophoblast giant cells (data not shown). At E9.5, embryos dissected from their decidua showed elevated levels of *mgcRacGAP* in the neuroepithelium of the brain ventricles and the neural tube, but overall, embryonic expression remained detectable (data not shown). X-gal staining of heterozygous *gtl11* embryos confirmed this expression pattern (Fig. 1C). At E12.5, the expression remained widespread. However, in the brain of E12.5 embryos (Fig. 1G), higher mRNA levels were observed in the ventricular zone of the two telencephalic lobes, and in the mesencephalon and diencephalon, with the exception of the median sulcus. A strong signal was observed in the pontine nucleus in the ventral part of the mesencephalon. Specific hybridization was also detected in the dorso-lateral part of the (sub)ventricular zone of the neural tube throughout the whole embryo (Fig. 1H), and elevated levels were seen in the olfactory epithelium (Fig. 1I), the vomeronasal (Jacobson's) organ, the vagus nerve and the thymic primordia. Similar observations were done in X-gal stained E12.5 embryos (Fig. 1D). In line with our findings, *mgcRacGAP* mRNA accumulation was observed in the cerebral cortex of the telencephalon and the medial and lateral ganglionic eminences of the mouse brain at E14.5 (Arar et al., 1999). Therefore, *mgcRacGAP* has a uniform expression pattern during the pre-organogenesis stages of development, but high mRNA levels are observed at specific sites from E9.5 onwards.

X-gal staining of adult brain showed the highest expression in the cerebellum, more specifically in the Purkinje cell layer extending into the molecular layer (Fig. 1J–L). Relatively high levels were also detected in other discrete brain regions, such as the hippocampus (strongest in CA3), the shell of the nucleus accumbens, the central amygdaloid nucleus, the habenular commissure and the piriform cortex. In the cortex, positive cells were scattered sparsely throughout all layers (data not shown).

Global *mgcRacGAP* expression in adult mice was analyzed using Northern blotting (Fig. 2). Two transcripts, likely due to differences in 3′-UTR (see above), were found in the spleen, lung, and testis. The expression was high in the testis and spleen, two tissues that maintain a high mitotic index during adult life. The expression in the heart, skeletal muscle and kidney was limited, and only the very faint, 3.1 kb-long transcript could be detected upon overexposure. Expression of neither of the two mRNA size classes could be detected in adult liver (unlike in the embryonic liver; data not shown).

2.3. Homozygous mgcRacGAP$^{gtl11/\beta geo}$ embryos are arrested during pre-implantation development

Heterozygous mutant mice were grossly phenotypically normal and fertile. Crosses between heterozygotes failed to yield any homozygous mutant animals among the offspring ($n = 27$ in Fig. 3A). This indicated that the insertion of the vector, which leads to a residual truncated mgcRacGAP protein moiety (after Ala62) in the encoded gtl11/βgeo fusion protein, caused an embryonic lethal recessive (and likely, total; see Section 3) loss-of-function mutation. To time the embryonic lethality, embryos of heterozygous crosses were dissected and genotyped by RT-PCR (Fig. 3B). Between E6.5 and E10.5, all embryos investigated were either wild-type or heterozygotes (Fig. 3D). This suggested that *mgcRacGAP* is already essential during pre- or peri-implantation. A peri-implantation defect was estimated by scoring spontaneous abortions (via detection of resorption sites) in the uteri of heterozygous and wild-type females, respectively, after mating with heterozygous males. In wild-type females, the frequency of naturally occurring resorptions was 4.2% (three out of 71). In heterozygous intercrosses, the frequency of resorption sites raised to 16.7% (13 out of 78), which is significant (Student's *t*-test; $P = 0.003$), though an increase to 25%, as expected if all knockout embryos would initiate implantation, was not observed. In situ hybridization for wild-type *mgcRacGAP*

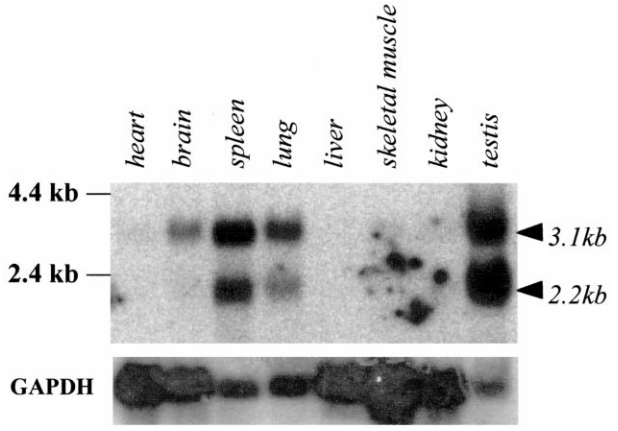

Fig. 2. Northern blot analysis of poly(A)-RNA from adult mouse organs. The blot was hybridized using a labelled 1.65 kb-long *Eco*RI cDNA fragment of EST clone 402177, which corresponds to 87% of the mgcRacGAP open reading frame (9–1740 bp, encoding for amino acid E30–F580). A GAPDH probe was used as the loading control.

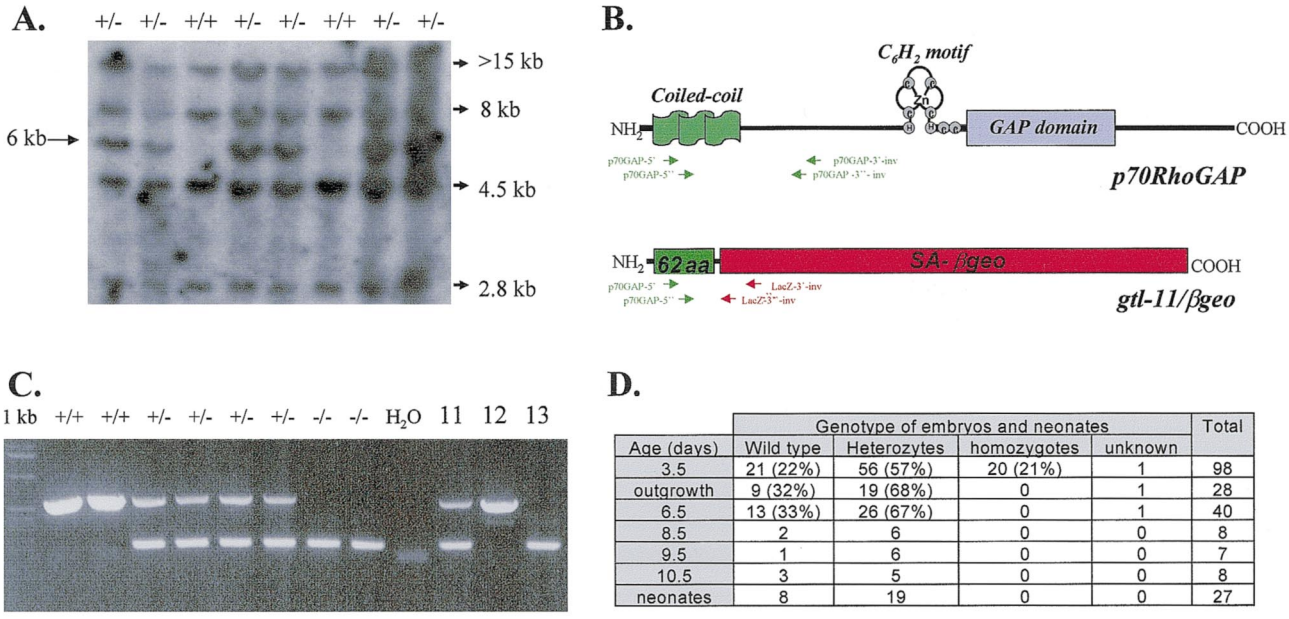

D.

	Genotype of embryos and neonates				Total
Age (days)	Wild type	Heterozytes	homozygotes	unknown	
3.5	21 (22%)	56 (57%)	20 (21%)	1	98
outgrowth	9 (32%)	19 (68%)	0	1	28
6.5	13 (33%)	26 (67%)	0	1	40
8.5	2	6	0	0	8
9.5	1	6	0	0	7
10.5	3	5	0	0	8
neonates	8	19	0	0	27

Fig. 3. Genotyping of offspring from heterozygous mouse mating. (A) Southern blot analysis of pups derived from heterozygous crosses. *Eco*RI-digested genomic DNA reveals a gene trap-diagnostic, extra 6 kb DNA fragment, that is absent in wild-type DNA when probing with the 1.65 kb-long *Eco*RI cDNA fragment of EST clone 402177. (B) RT-PCR strategy for genotyping pre-implantation embryos; approaches for the wild-type (top) and *gtl-11* (lower) alleles are illustrated. Two 3′ primers (one *LacZ* (red) and one *mgcRacGAP*-specific (green)) were combined with one *mgcRacGAP*-specific 5′ primer in the first PCR amplification (5′ and 3′) and the nested PCR amplification (5″ and 3″). The wild-type allele yields a 606 bp-long fragment, a mutated allele, a 172 bp-long fragment. (C) PCR-based genotyping results: (lane 1), 1 kb DNA marker; (lanes 2–9), PCR products obtained using the described combination of three primers on wild-type, and heterozygous and homozygous mutant blastocysts; (lane 10), water was used as a negative control. (Lanes 11–13) PCR products obtained using: (lane 11), the combination of three primers on RNA from *gtl11* ES cells; (lane 12), only *mgcRacGAP*-specific primers (5′ and 3′); and (lane 13), by combining the *LacZ*-specific and the *mgcRacGAP* 5′-specific primers. (D) Genotype distribution of embryos and pups derived from heterozygous intercrosses. The percentages corresponding to the genotypes are given between parentheses. See Section 4 for practical details on the blastocyst outgrowth assays in vitro.

mRNA was performed at E6.0 on 22 decidua from heterozygous intercrosses. Twenty contained embryos that had a normal size, gross morphology and *mgcRacGAP* mRNA expression pattern. The two other decidua were empty, and no remnants of implanted embryos could be detected (data not shown). To correlate the homozygous mutant genotype with a late pre-implantation phenotype, 97 blastocyst-stage embryos (E3.5) were collected from heterozygous intercrosses. Fig. 3B outlines the RT-PCR genotype strategy and Fig. 3C depicts the results of a typical experiment. At this stage, the three possible genotypes were recovered in the expected Mendelian ratio (Fig. 3D). In this setup, the complete absence of a PCR product indicative for the wild-type allele in the homozygous knockout blastocysts excludes the presence of wild-type mRNA transcripts by splicing around the gene trap insertion.

Next, uterine implantation of blastocysts was simulated by explanting E3.5 embryos individually on fibronectin-coated plates. During the first 48–72 h, 84% (43 out of 50) of the blastocysts derived from appropriate control matings hatched from the zona pellucida. They attached to the substrate and trophoblast giant cells grew out, with a clump of cells on top derived from the inner cell mass. Homozygous mutant embryos could hatch in vitro, but the number of embryos from heterozygous intercrosses that showed a trophoblast outgrowth from after 72 to even 96 h, dropped to 54% (28 out of 52). Normal looking outgrowths (at 96 h) in the latter experiment were then genotyped (Fig. 3D): 19 embryos were heterozygous and nine embryos were wild-type. This is consistent with a recessive lethal allele.

2.4. Cellular defects in mgcRacGAP homozygous mutant blastocysts

Close inspection of the mutant blastocysts, initially in expanded blastocysts and afterwards in earlier embryos (E3.0–3.5), gave important clues as to the function of mgcRacGAP in mouse embryogenesis. Although all E3.5–4.0 embryos collected from heterozygous intercrosses displayed a quasi uniform size, homozygous mutant embryos exhibited a dramatically abnormal morphology (Fig. 4A,B). Interestingly, whereas heterozygous and wild-type blastocysts typically contained 40–60 cells (Fig. 4B), the homozygous mutant blastocysts consisted of only a few enlarged cells (on average, only 3–6; Fig. 4A). These expanded cells appeared stretched with smooth surfaces. The embryos with smaller cell numbers were not true blastocysts, since no inner cell mass was observed. Confocal microscopy revealed that the mgcRacGAP homozygous mutant blastocysts contained greatly enlarged and elongated nuclei (TOPRO-3 staining; Fig. 4H,I). Given the well-estab-

lished role of Rho proteins in the regulation of the actin cytoskeleton, we examined the location and appearance of the actin network in mutant blastomeres. No aberrant accumulation or redistribution of actin cytoskeleton, as assayed by phalloidin–FITC staining, was observed in blastocyst-stage embryos within the resolution of this technique. E4.0 embryos displaying the mutant phenotype were very fragile and collapsed easily when freed from their zone pellucida.

The presence of few and enlarged cells in mutant expanded blastocysts prompted us to examine them at earlier stages. Wild-type morulae develop into blastocysts (E3.5) containing regularly sized cells and nuclei (Fig.4E,G). In contrast, *mgcRacGAP* homozygous mutants were abnormal in morphology. Phalloidin–FITC labelling demonstrated that such morulae contained, on average, only 3–6 cells/embryo (Fig. 4C,D,F). They differed from normal four-cell stage embryos by the compacted appearance of the blastomeres, the occurrence of cavitation (although sometimes limited; Fig. 4F), and their free-floating presence in the uterus. Multinucleated blastomeres were frequently observed among the blastomeres in these homozygous mutant embryos, suggesting that appropriate completion of cell division is inhibited. The nuclei were generally larger than normal, and two nuclei within one blastomere were often partially connected (Fig. 4C). Cortical actin staining lined the affected compacted blastomeres, with a more intense staining at regions of cell–cell contact. Occasionally, actin clustering was observed at particular sites in these early embryos (e.g. around the incipient cavitations) or a partial cytokinetic actin furrow could be observed in blastomeres (Fig. 4D).

Interestingly, Jantsch-Plunger et al. (2000) recently analyzed in *C. elegans* the phenotype caused by a subtle missense mutation in *CYK-4*. CYK-4 protein contains a conserved GAP domain that is specific for Rho-like GTPases, and is the *C. elegans* orthologue of mgcRacGAP. The primary phenotype is the failure to assemble the midzone microtubules during late stages of cytokinesis. This suggests that mgcRacGAP is a conserved protein, and that it may have a similar function in mouse embryogenesis.

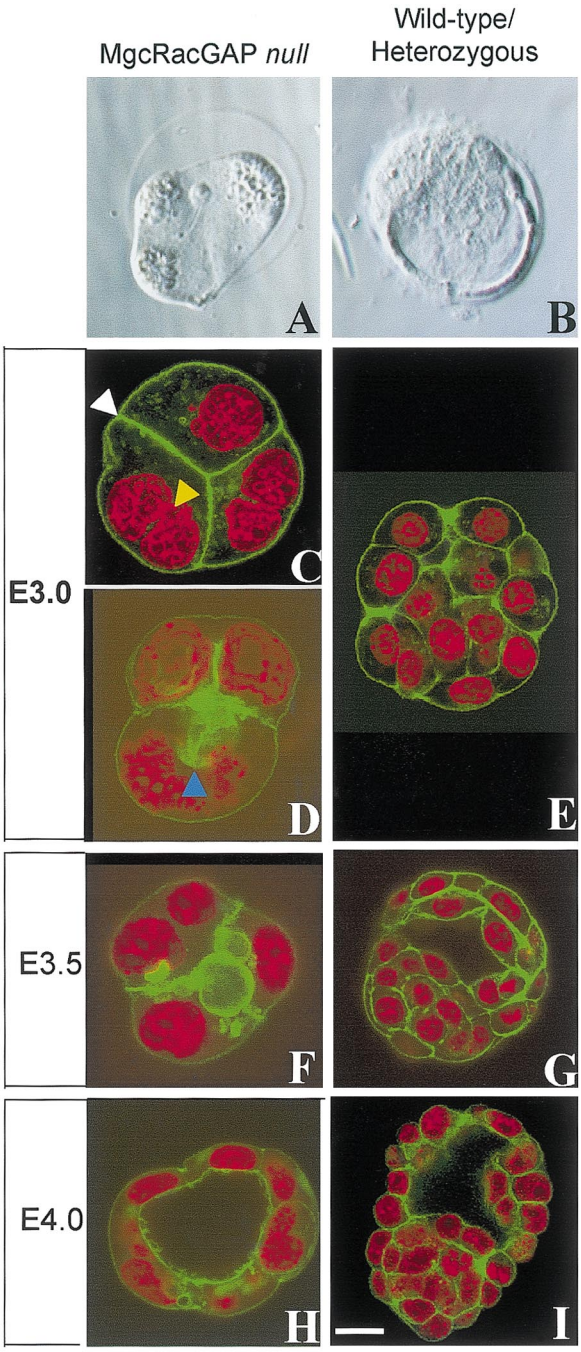

3. Discussion

A gene trap screen in ES cells has been designed and used to identify and mutate genes that are essential for normal embryogenesis and to document their expression pattern. In doing so, we generated a recessive and embryonic lethal mutation in *mgcRacGAP*, which, during the course of this

Fig. 4. Pre-implantation phenotype in E3.0–E4.0 *mgcRacGAP null* embryos. (A) E3.5–E4.0 *mgcRacGAP null* embryo containing only a few giant blastomeres with a stretched appearance. (B) At this stage, normal embryos have acquired a typical blastocyst-stage morphology and cell number. (C–I) The embryos were double-stained for the presence of actin (FITC–phalloidin; green) and the nucleus (TOPRO-3; red), and analyzed by confocal microscopy. The left panel shows phenotypic mgcRacGAP *null* embryos, the right panel shows normal control embryos of a similar stage. (C–E) E3.0–3.5 embryos in panels (C) and (D) have the appearance of abnormal (i.e. delayed) compacted morulae. The phalloidin–FITC labelling demonstrates the presence of only three blastomeres, but their nuclei are enlarged, and the blastomeres are binucleated. Note the compacted appearance of the blastomeres (white arrowhead), the internuclear connection (yellow arrowhead) and the abrogated cytokinetic actin furrow (blue arrowhead). Embryo (F) has initiated cavitation. (H) Aberrant expanded E4.0 embryo. The blastomeres of such embryos, as well as the nuclei, have a stretched morphology. All blastomeres are multinucleated. (I) Wild-type E4.0 embryo. (C–I) Bar, 25 μm.

work, appeared to be the murine homologue of *C. elegans* CYK-4, a Rho GAP, that was shown recently to be essential for central spindle assembly and late steps of cytokinesis in *C. elegans* (Jantsch-Plunger et al., 2000). Though the gene trap vector insertion in the mgcRacGAP allele resulted in a truncated protein that only contains the first 62 amino acids, this residual truncated polypeptide fused to the β-geo reporter might still exert some residual function. At present, however, we consider the homozygous mutant embryos arbitrarily as *null* mutants. We analyzed the phenotype of homozygous embryos of the mutant allele of the *mgcRacGAP* gene, and found this gene to be essential soon after conception. Homozygous mutant *MgcRacGAP* blastocysts displayed a dramatic reduction in cell number, but underwent compaction and formed a blastocoel. Multinucleated blastomeres with partially formed cleavage furrows could be observed. This phenotype suggests that the mouse protein has retained a similar function during cytokinesis as has been described for the *C. elegans* orthologue, CYK-4. However, an additional phenotype to the CYK-4 (*t1689ts*) mutant phenotype in worms is that the different nuclei in knockout mouse blastomeres often remain interconnected.

3.1. Predicted structure of mgcRacGAP

Three domains can be discriminated within the RhoGAP proteins. The C-terminal half of the protein contains the catalytic GAP^{Rho} domain, a C_6H_2 motif flanks the binding site for the GTPase and the N-terminal segment of mgcRacGAP is likely to adopt a coiled-coil structure. Although the role of the latter two domains remains to be established, they are probably of functional importance because both domains and their position with respect to the GAP^{Rho} domain are evolutionary conserved from worm over fly to mouse and man. The isolation of candidate partners for each of these subdomains will therefore provide new insights into intracellular mgcRacGAP function. Probably amongst these are members of the MKLP1-subfamily of kinesin-like protein, as even a subtle mutation in the extreme N-terminal segment of CYK-4 in *C. elegans* leads to mislocalization of ZEN-4 protein (Jantsch-Plunger et al., 2000).

The GAP domain of human MgcRacGAP and CYK-4 have, in vitro, the highest specificity towards Rac1 and Cdc42 (Touré et al. 1998; Kawashima et al., 2000; Jantsch-Plunger et al., 2000). As for the majority of RhoGAPs, it remains at present unclear what is the real in vivo target for mgcRacGAP in the pre-implantation mouse embryo. Hints may come from conceptually different studies in other cell culture systems or species. Inhibition and constitutive activation of either RhoA or Cdc42 inhibits normal constriction of the cleavage furrow in *Xenopus* embryos, thereby blocking cytokinesis (Drechsel et al., 1997). Likewise, the injection of constitutively activated V12Cdc42 protein in newly formed four-cell mouse embryos leads to a reversion of cytokinesis, producing cells that continue nuclear division, but do not proceed to cytokinesis (Clayton et al., 1999). Polyploidy can result from interference with Rho GTPase activity, since treatment with C3 toxin, which specifically ADP ribosylates Rho GTPase, results in multinucleated giant cells in fertilized eggs of *Xenopus laevis* (Kishi et al., 1993) and the sea urchin (Mabuchi et al., 1993), as well as in cultured animal cells (Rubin et al., 1988). Similarly, expression of dominant negative or oncogenic mutants of Ect2, a Rho-specific exchange factor with a role in the regulation of cytokinesis, results in an increase in binucleated hepatocytes (Sakata et al., 2000). These findings indicate that RhoA and Cdc42 have a role in cytokinesis in higher eukaryotes. However, gene targeting experiments in the mouse showed that Cdc42 is not essential for viability or proliferation of mammalian early embryonic cells (Chen et al., 2000). Similarly, Rac1 is unlikely to be the in vivo target for mgcRacGAP since Rac1-deficient mice are gastrulation-defective but without signs of multinucleated cells, which would be indicative of a cytokinesis defect (Sugihara et al., 1998).

3.2. The presence of multinucleated cells in the null embryos suggests a role for mgcRacGAP in cell division

Since *null* mutant mouse embryos successfully complete the first two cell divisions, it can be assumed that the egg provides sufficient maternal mRNA and/or protein for up to three cell division cycles. Maternally derived mRNA in the mouse is generally degraded rapidly upon activation of the zygotic genome at the two-cell stage (Flach et al., 1982). Without further replenishment from the maternal pool, *mgcRacGAP* deficiency soon manifests itself as a cell division problem in the mouse embryo, as indicated by the presence of larger nuclei and bi-nucleated blastomeres.

At which stage does mgcRacGAP function in cell division? Interestingly, the phenotypic analysis of a *C. elegans* mutant in the *CYK-4* gene was reported during the course of this work. Based on their work, Jantsch-Plunger et al. (2000) convincingly attributed a role for CYK-4 protein in the assembly of the central spindle and, as a consequence, for the intrusion of the contractile ring. Given the sequence homology of mgcRacGAP with CYK-4, their structural similarity, and the observation of bi-nucleated blastomeres and abrogated cleavage furrows in both mutant embryos, mgcRacGAP is likely to have a similar role in the late steps of cytokinesis, i.e. the assembly of the central spindle. However, our observation of internuclear connections suggests that (primarily the third) nuclear division and/or nuclear assembly during cell division is also not completed in the *mgcRacGAP*-deficient mouse embryos. This phenotype points towards an additional function of mgcRacGAP in the mitotic spindle. Apparently, during early cleavage, mitosis proceeds essentially to completion, and results in nuclear membrane reformation around each of the two fully separated chromatid masses before cytokinesis ensues cell division. Along with the fading of the maternal transcript and its translated product, chromosome segregation

becomes increasingly aberrant. We propose that the bulk of sister chromatids still initiate polar separation, but complete segregation to the poles is not achieved and results in decondensed chromosomes tethering around the central midzone. Eventually, during the default telofase, the nuclear envelope would then reform around each of the two poorly separated chromatid masses, but resulting in internuclear connections. The observation that nuclei of knockout mouse embryos are significantly larger in size compared with normal nuclei suggests further that replicated chromosomes have also failed to segregate later on, leading to a nuclear membrane being reformed around a multiploid genome.

This additional phenotype in our gene trap mouse, as compared with the phenotype in *C. elegans*, may be due to the fact that the gene trap vector integration leads to a truncated mgcRacGAP protein (after Ala62) in the encoded gtl11/βgeo fusion protein, thereby abolishing a large part of the coiled-coil domain, as well as the complete C_6H_2 domain and the catalytic GAP domain. In contrast, the CYK-4 temperature-sensitive (t1689ts) *C. elegans* mutant has a point mutation leading to S15L substitution in the *CYK-4* gene, leaving the C_6H_2 and GAP domains unaffected.

From the cell biological observations in the *C. elegans* mutants, it was speculated that the N-terminal part of CYK-4 may act to promote central spindle assembly, since the integrity of the ultimate N-terminal segment of the protein is essential for correct localization of ZEN-4. This would then be independent of CYK-4's GAP activity. From the analysis of the nuclei of mgcRacGAP-deprived embryos, we suggest that the normal protein, independently as to whether this includes the GAP domain, plays a role during earlier steps of cell division and is a prerequisite for correct chromosome segregation. Supporting evidence for such a function comes from the observation that the CYK-4 protein localizes around the mitotic spindle when *C. elegans* cells enter mitosis.

3.3. The lethal embryonic phenotype

Rho and Cdc42 GTPase cycles are involved in the initiation of morphological changes in blastomeres and the maintenance of their polarization (Clayton et al., 1999), one of the earliest signs of cell specialization in the embryo. This involves, amongst others, the formation of apical membrane microvilli and redistribution of the actin cytoskeleton (Fleming and Johnson, 1988). The onset of expression of *mgcRacGAP* coincides with the induction of polarity in a subset of blastomeres of the eight-cell embryos (Johnson and Ziomek, 1981; Ziomek and Johnson, 1980). Although aberrant mouse embryos contain fewer cells than normal and may have an increased ploidy, the mechanisms underlying cell polarization, compaction and cavitation appear unaffected in the absence of *mgcRacGAP*. The undisturbed compaction of these embryos therefore suggests that mgcRacGAP is not essential for the initiation or maintenance of the polarization of mouse blastomeres, since this is a requisite for subsequent compaction. Thus, the compaction and cavitation seen here occur apparently independent of the absolute cell number, which is in agreement with previous studies showing that artificially created tetraploid (Ozil and Modlinski, 1986; Kubiak and Tarkowski, 1985), octaploid (Winkel and Nuccitelli, 1989) and bisected (Wang et al., 1990) embryos divide and cavitate on schedule. MgcRacGAP *null* embryos are able to hatch in vitro from the zona pellucida in synchrony with wild-type and heterozygous embryos, and reach an expanded blastocyst-like stage, although without apparent inner cell mass.

Given the early cleavage stages at which the *null* mouse embryos stop dividing, it is not completely unexpected that these embryos failed to attach in vitro and to grow out on fibronectin-coated substrates, an assay that has been proposed to reflect the earliest steps of trophoblastic invasion. However, in vivo, a significant number of knockout embryos apparently still implant, as reflected by the substantial increase in resorption sites that was observed upon heterozygous intercrossing versus the mating between a wild-type female and a heterozygous *gtl11* male. This may indicate that *mgcRacGAP*-deficient blastomeres lining the blastocyst cavity can behave as trophoblast cells and attach to the uterine wall, but this is not followed by invasive proliferation. Alternatively, dying or dead (but previously hatched) expanded blastocysts-like embryos may still induce decidual swelling by mechanical stress on the receptive uterus (McLaren, 1969).

The early lethality of mgcRacGAP-deficient embryos restricted our analysis to the very early pre-implantation stages and prohibited studies aiming towards documenting a role for mgcRacGAP in individual cell motility and substrate attachment. Even the derivation of ES cell lines from the homozygous mutant embryos for further in vitro studies is impossible. In addition to the crucial function of mgcRacGAP in cytokinesis, the protein may be relevant to later stages of embryogenesis and adult life. Given the resemblance to MgcRacGAP and CYK-4, it may function in spermatogenesis and the female germ-line (Touré et al., 1998; Jantsch-Plunger et al., 2000; Arar et al., 1999). The specific localization of the gtl11–βgeo fusion protein in defined regions of the developing central nervous system from E9.5 onwards suggests that this protein functions in the nervous system. This is in line with the uncoordinated behaviour of CYK-4 temperature-sensitive *C. elegans* mutants (Jantsch-Plunger et al., 2000) and the postulated role for Rho-like GTPases in neuron outgrowth and migration (Jalink et al., 1994; Luo et al., 1994; Zipkin et al., 1997). *MgcRacGAP* shares the adult brain expression domain with other GAP^{Rho}-containing genes like Myr7 (Chieregatti et al., 1998), n- and α-chimerin (Hall et al., 1990, 1993) and bcr (Fioretos et al., 1995). In addition, mutations in *oligophrenin-1*, another RhoGAP, are responsible for X-linked, non-specific mental retardation (Billuart et al., 1998). Studies on the role of mgcRacGAP in processes like axon outgrowth, neuronal plasticity, synapto-

genesis, as well as specific neuronal signalling pathways, then seem to be targets for the future, but will have to be carried out in the mouse in a different setting than this gene trap context.

Taken together, the findings in *C. elegans* (Jantsch-Plunger et al., 2000) and our observations in the mouse in vivo, provide evidence that the protein orthologues (CYK-4, CG13345, mgcRacGAP and MgcRacGAP) are essential in several microtubule-dependent steps during mitosis and that this machinery is conserved throughout evolution. In contrast with the subtle point mutation in *C. elegans*, the absence of the protein may interfere with the functioning of the mitotic spindle in segregating chromosomes and proper completion of nuclear fission. Subsequently, the protein is essential in central spindle formation, a prerequisite for the completion of cytokinesis. In addition, the severe phenotype of *null* embryos indicates that *mgcRacGAP* is functionally non-redundant and cannot be substituted by other GAPs.

4. Experimental procedures

4.1. Cell culture and generation of mice

RW4 ES cells (Genome Systems, Inc.) were co-cultured with growth-inhibited primary embryonic fibroblasts, prepared from pEPIL4 transgenic embryos (W. Müller, Institute of Genetics, University Köln; Wurst and Joyner, 1993). ES cells (6×10^6 cells) were electroporated (250 V, 450 μF, 99 Ω) with 30 μg linearized pSAβgeo, and cell clones were selected in 200 μg G418/ml (Geneticin, GIBCO BRL) for 5 days. *Gtl11* ES cells were used to generate chimeras by a modified ES cell-diploid aggregation protocol (Wood et al., 1993), using a single morula-stage FVB/N embryo, and the embryos were reintroduced into the uterus of pseudo-pregnant CD1 females. Resulting chimeric males that transmitted the mutation through the germ-line were bred to C57Bl/6 mice. The results presented here are obtained with transgenic animals that were backcrossed over three or more generations.

4.2. Genotyping and staining of embryos and adult mice

Genomic DNA was prepared from ES cells and mouse tail biopsies according to standard procedures. For genotyping of embryos, DNA was purified from the yolk sac, and then analyzed by Southern blotting or PCR. In pSAβgeo transgenes, Southern blotting of *Bam*HI-digested DNA (Sambrook et al., 1989) reveals a 3 kb band that is recognized by the [α^{32}P]dCTP labelled probe (the first 800 bp of *E. coli LacZ*). Pre-hybridization of the membranes and hybridization were at 60°C using Quickhyb (Stratagene). Following hybridization, the membranes were washed in 0.5 × SSC, 0.1% SDS at 60°C. PCR-based screening of pSAβgeo mice was done according to Hanley and Merlie (1991). X-gal staining for βgal activity of ES cells and embryos was according to Gossler and Zachgo (1993).

4.3. Cloning of mgcRacGAP/βgeo fusion cDNA

We used a 5′-RACE kit (Gibco-BRL), cDNA synthesis (using *LacZ*-specific primer, 5′-TGCATCTGCCAGTTTGAGGGG-3′) and the addition of the homopolymeric-dC tail, all as proposed by the manufacturer. The first PCR (25 cycles) was done at an annealing temperature of 55°C in reaction mixture (1× goldstar reaction buffer supplemented with 2.5 mM $MgCl_2$, 250 μM of each dNTP) with 1 μM each of 5′-RACE abridged anchor primer (AAP; Gibco-BRL) and 5′-CGGGATCCGCCATGTCACAGA-3′ on *gtl11* ES cell RNA. A 1:100 diluted sample of the first PCR was used for nested PCR (32 cycles; reaction mixture with 1 μM each of primers AAP and M13/pUC Forward(-40) (Promega); annealing at 60°C). The PCR products were separated on an agarose gel and discrete bands were extracted using Qiaex (Westburg) and directly subjected to sequencing (ABI PRISM, Perkin–Elmer).

4.4. Cloning of wild-type mgcRacGAP cDNA

The EST clone, 402177, was obtained from the IMAGE consortium (http://bbrp.llnl. gov/bbrp/image) and sequenced. Due to the fact that heterozygous E12.5 embryos produce βgal, we screened an in-house made E12.5 CD1 embryo cDNA library (Verschueren et al., 1999) in order to obtain both 3′ splice forms. A 1.6 kb-long *Eco*RI cDNA fragment of EST402177 was used as a probe. Three different positive clones appeared to be derived from splicing variant B, which differs in its 3′-UTR from the EST clone 402177 (variant A). Based on the determined sequences, additional EST clones (cDNA clones 721331 (variant A); 577676 (A); 640147 (A); 575409 (B); 475329 (B); 764336 (B); 387228 (B); 373125(B)) were obtained, and sequenced.

5′-RACE was performed to obtain the missing sequences. The first PCR (25–35 cycles) was done with annealing at 55°C, reaction mixture as above, and 10 μM of 5′-TTGGTTCTTTGATACTTCTTTCGG-3′, which is a *gtl11*-specific sequence shared by all 5′ splice variants. A 10-fold diluted sample of the first PCR products was used for a nested PCR using 10 μM of primer 5′-CTCCATCCGGCGCACAAGCTGC-3′ (35 cycles; annealing at 60°C). Fragments were separated on a gel, extracted using Qiaex (Westburg), cloned in PCRscriptII (Westburg) and sequenced.

4.5. Northern blot analysis

Northern blots with poly(A)-RNA (2 μg/lane) from adult mouse tissues were from Clontech. The DNA probes were radiolabeled by random priming. Hybridization was done overnight at 60°C using Quickhyb (Stratagene). After hybridization, two washes were applied (60°C; in 2× SSC, 0.1% SDS; 30 min each).

4.6. Allele-specific genotyping of gtl11 embryos by RT-PCR

Pre-implantation stage embryos were obtained by flushing the oviducts, and the embryos were cultured in M16 medium. Individual embryos were transferred to 5 μl DEPC-treated water, supplemented with 1 U RNasin/μl (Promega). E6.5 embryos were dissected free from decidual tissue and transferred to 35 μl DEPC-treated water. The samples were immediately frozen on dry ice and stored at −80°C until use. The embryos were lysed by repeated cycles of thawing and freezing; the number of cycles equals the age in days of the embryo. The lysate was then diluted by addition of the components of the Superscript™ Preamplification system (Gibco-BRL) and RNasin (1 U/μl).

The first strand cDNA was generated with primers 5′-GCCTCCAGTATTCTGAGGTGTGCCCAAATTGTCTGTGTCAG-3′ (p70GAP-3′-inv) and 5′-GCCAGTTTGAGGGGACGACGACAGTATCGGCC-3′ (LacZ-3′-inv) specific for the wild-type *mgcRacGAP* allele and *E. coli LacZ*.

The first PCR (35 cycles) was then carried out with one-fourth of the cDNA. The annealing temperature was 65°C; $MgCl_2$ was adjusted to 2.5 mM, and 1 μM of each primer (5′-GGACTCTGTTTGAGCAGCTTGTGCGCCGGATGGAG-3′ (p70GAP-5′), p70GAP-3′-inv- and *LacZ*-3′-inv) was used. A 1 μl sample of this PCR was used in a second PCR (35 cycles, annealing at 60°C) that combined two nested *mgcRacGAP*-specific primers (5′-GATTCATTTGCCTGGTCTAC-3′ (p70GAP-3″-inv) and 5′-GCAGCTTGTGCGCCGGATGGAG-3′ (p70GAP-5″)) and one *LacZ*-specific primer (M13/pUC Forward(-40) (Promega), i.e. LacZ-3″-inv; 1 μM). The *mgcRacGAP* wild-type allele product is amplified by a combination of primers p70GAP-3″-inv and p70GAP-5″, and is 606 bp long. The product amplified by the combination of p70GAP-5″ and LacZ-3″-inv, and derived from the mutated allele, is 172 bp long.

4.7. Genomic localization of mgcRacGAP

Genomic localization of *mgcRacGAP* was performed using radiation hybrids as previously described (Kozak et al., 1990)

4.8. Blastocyst outgrowth in vitro

Heterozygous and wild-type littermate females were mated with heterozygous mutant males, and the embryos were isolated (E3.5), and cultured individually in 10 μl ES cell medium without LIF (Wurst and Joyner, 1993) in Terasaki wells (Greiner) that were coated at 4°C with human plasma fibronectin (Gibco-BRL, 1 μg/μl in PBS). The plate was kept in a humid chamber at 37°C, 5% CO_2, and the embryonic outgrowth was scored daily. Every other day, 5 μl of fresh medium was added to the wells. On the fourth day, the cultures were washed briefly in PBS, and the embryos were lysed in 6 μl DEPC-treated water. The samples were then genotyped (see above).

4.9. In situ hybridization

In situ hybridization was done according to Dewulf et al. (1995), using a specific *mgcRacGAP* RNA probe encompassing 705–1081 bp.

4.10. Phalloidin and TOPRO-3 staining of pre-implantation stage embryos

The embryos (E3.5) were isolated and the zona pellucida was removed with Acid Tyrode solution. The embryos were transferred to chambers (Hyman et al., 1984) and were fixed for 30 min in 1.7% paraformaldehyde in PBS, permeabilized for 10 min with 1% Triton X-100 in PBS, and incubated overnight with phalloidin–FITC (2 μg/ml; Sigma) in PBS with 1% Tween20 and 3% bovine serum albumin at 4°C. The embryos were washed three times in PBS with 1% Tween20, and incubated for 15 min in washing buffer containing 10 μM TOPRO-3 (Molecular Probes) for nuclear staining. The embryos were then embedded in Vectashield (Vector) and analyzed by confocal laser scanning microscopy.

4.11. X-gal staining on adult brain sections

Adult mice were anaesthetized with pentobarbital and perfused transcardially with saline, followed by ice-cold 1% formaldehyde and 0.2% glutaraldehyde in PBS containing 2 mM $MgCl_2$ for 15 min. Coronal brain sections (100 and 200 μm) were cut at 4°C, and stained in X-gal (1 mg/ml) staining solution prepared in 5 mM K-ferricyanide, 5 mM K-ferrocyanide and 2 mM $MgCl_2$. The sections were stained at 37°C for 24 h. After staining, the sections were fixed with 4% paraformaldehyde. The sections were mounted on gelatin-coated slides, and in some cases, counterstained with Cresyl Violet.

Acknowledgements

The authors are grateful to E. Joris for animal care, to H. Alexandre, S. Pampfer, A. Van Cauwenberge, J.J. Goval and W. Annaert for discussions and help with immunofluorescence, to P. Tylzanowski and N. De Wulf for 5′-RACE expertise. The authors also thank G. Friedrich and P. Soriano for providing the vector pSAβgeo. The work in the DH lab was supported by infrastructural funding (COT-023), VIB (VIB-07) and FWO-V (project G.0165.96). TVdP and OL were supported by a pre-doctoral IWT and post-doctoral FWO-V fellowship, respectively, and VB and AZ were supported by a FWO-V post-doctoral fellowship during part of this work.

References

Arar, C., Ott, M.O., Toure, A., Gacon, G., 1999. Structure and expression of murine mgcRacGAP: its developmental regulation suggests a role for

the Rac/MgcRacGAP signalling pathway in neurogenesis. Biochem. J. 343, 225–230.

Billuart, P., Bienvenu, T., Ronce, N., des Portes, V., Vinet, M.C., Zemni, R., Crollius, H.R., Carrie, A., Fauchereau, F., Cherry, M., Briault, S., Hamel, B., Fryns, J.P., Beldjord, C., Kahn, A., Moraine, C., Chelly, J., 1998. Oligophrenin-1 encodes a rhoGAP protein involved in X-linked mental retardation. Nature 392, 923–926.

Boguski, M.S., McCormick, F., 1993. Proteins regulating Ras and its relatives. Nature 366, 643–654.

Chen, F., Ma, L., Parrini, M.C., Mao, X., Lopez, M., Wu, C., Marks, P.W., Davidson, L., Kwiatkowski, D.J., Kirchhausen, T., Orkin, S.H., Rosen, F.S., Mayer, B.J., Kirschner, M.W., Alt, F.W., 2000. Cdc42 is required for PIP(2)-induced actin polymerization and early development but not for cell viability. Curr. Biol. 10, 758–765.

Chieregatti, E., Gartner, A., Stoffler, H.E., Bahler, M., 1998. Myr 7 is a novel myosin IX-RhoGAP expressed in rat brain. J. Cell Sci. 111, 3597–3608.

Clayton, L., Hall, A., Johnson, M.H., 1999. A role for Rho-like GTPases in the polarization of mouse eight-cell blastomeres. Dev. Biol. 205, 322–331.

Dewulf, N., Verschueren, K., Lonnoy, O., Moren, A., Grimsby, S., Vande Spiegle, K., Miyazono, K., Huylebroeck, D., ten Dijke, P., 1995. Distinct spatial and temporal expression patterns of two type I receptors for bone morphogenetic proteins during mouse embryogenesis. Endocrinology 136, 2652–2663.

Drechsel, D.N., Hyman, A.A., Hall, A., Glotzer, M., 1997. A requirement for Rho and Cdc42 during cytokinesis in *Xenopus* embryos. Curr. Biol. 7, 12–23.

Fioretos, T., Voncken, J.W., Baram, T.Z., Kamme, F., Groffen, J., Heisterkamp, N., 1995. Regional localization and developmental expression of the BCR gene in rodent brain. Cell. Mol. Biol. Res. 41, 97–102.

Fishkind, D.J., Silverman, J.D., Wang, Y.L., 1996. Function of spindle microtubules in directing cortical movement and actin filament organization in dividing cultured cells. J. Cell Sci. 109, 2041–2051.

Flach, G., Johnson, M.H., Braude, P.R., Taylor, R.A., Bolton, V.N., 1982. The transition from maternal to embryonic control in the two-cell mouse embryo. EMBO J. 1, 681–686.

Fleming, T.P., Johnson, M.H., 1988. From egg to epithelium. Annu. Rev. Cell. Biol. 4, 459–485.

Friedrich, G., Soriano, P., 1991. Promoter traps in embryonic stem cells: a genetic screen to identify and mutate developmental genes in mice. Genes Dev. 5, 1513–1523.

Gossler, A., Zachgo, J., 1993. Gene and enhancer trap screens in ES cell chimeras. In: Joyner, A.L. (Ed.). Gene Targeting: A Practical Approach, IRL Press, Oxford, pp. 181–225.

Gossler, A., Joyner, A.L., Rossant, J., Skarnes, W.C., 1989. Mouse embryonic stem cells and reporter constructs to detect developmentally regulated genes. Science 244, 463–465.

Hall, A., 1994. Small GTP-binding proteins and the regulation of the actin cytoskeleton. Annu. Rev. Cell. Biol. 10, 31–54.

Hall, C., Monfries, C., Smith, P., Lim, H.H., Kozma, R., Ahmed, S., Vanniasingham, V., Leung, T., Lim, L., 1990. Novel human brain cDNA encoding a 34 000 Mr protein n-chimerin, related to both the regulatory domain of protein kinase C and BCR, the product of the breakpoint cluster region gene. J. Mol. Biol. 211, 11–16.

Hall, C., Sin, W.C., Teo, M., Michael, G.J., Smith, P., Dong, J.M., Lim, H.H., Manser, E., Spurr, N.K., Jones, T.A., Lim, L., 1993. Alpha 2-chimerin, an SH2-containing GTPase-activating protein for the ras-related protein p21rac derived by alternate splicing of the human n-chimerin gene, is selectively expressed in brain regions and testes. Mol. Cell. Biol. 13, 4986–4998.

Hanley, T., Merlie, J.P., 1991. Transgene detection in unpurified mouse tail DNA by polymerase chain reaction. BioTechniques 10, 56.

Hill, C.S., Wynne, J., Treisman, R., 1995. The Rho family GTPases RhoA, Rac1, and CDC42Hs regulate transcriptional activation by SRF. Cell 81, 1159–1170.

Hyman, A.A., Glotzer, M., Johnson, M.H., Maro, B., 1984. The distribution of cytoplasmic actin in mouse 8-cell blastomeres. J. Embryol. Exp. Morphol. 82, 97–117.

Jalink, K., van Corven, E.J., Hengeveld, T., Morii, N., Narumiya, S., Moolenaar, W.H., 1994. Inhibition of lysophosphatidate- and thrombin-induced neurite retraction and neuronal cell rounding by ADP ribosylation of the small GTP-binding protein Rho. J. Cell Biol. 126, 801–810.

Jantsch-Plunger, V., Gonczy, P., Romano, A., Schnabel, H., Hamill, D., Schnabel, R., Hyman, A.A., Glotzer, M., 2000. CYK-4: a Rho family GTPase activating protein (GAP) required for central spindle formation and cytokinesis. J. Cell Biol. 149, 1391–1404.

Johnson, M.H., Ziomek, C.A., 1981. Induction of polarity in mouse 8-cell blastomeres: specificity, geometry, and stability. J. Cell Biol. 91, 303–308.

Joyner, A.L., Auerbach, A., Skarnes, W.C., 1992. The gene trap approach in embryonic stem cells: the potential for genetic screens in mice. Ciba Found. Symp. 165, 277–288.

Kawashima, T., Hirose, K., Satoh, T., Kaneko, A., Ikeda, Y., Kaziro, Y., Nosaka, T., Kitamura, T., 2000. MgcRacGAP is involved in the control of growth and differentiation of hematopoietic cells. Blood 96, 2116–2124.

Kishi, K., Sasaki, T., Kuroda, S., Itoh, T., Takai, Y., 1993. Regulation of cytoplasmic division of *Xenopus* embryo by rho p21 and its inhibitory GDP/GTP exchange protein (rho GDI). J. Cell Biol. 120, 1187–1195.

Kozak, C.A., Peyser, M., Krall, M., Mariano, T.M., Kumar, C.S., Pestka, S., Mock, B.A., 1990. Molecular genetic markers spanning mouse chromosome 10. Genomics 8, 519–524.

Kubiak, J.Z., Tarkowski, A.K., 1985. Electrofusion of mouse blastomeres. Exp. Cell. Res. 157, 561–566.

Lamarche, N., Hall, A., 1994. GAPs for rho-related GTPases. Trends Genet. 10, 436–440.

Luo, L., Liao, Y.J., Jan, L.Y., Jan, Y.N., 1994. Distinct morphogenetic functions of similar small GTPases: *Drosophila* Drac1 is involved in axonal outgrowth and myoblast fusion. Genes Dev. 8, 1787–1802.

Mabuchi, I., Hamaguchi, Y., Fujimoto, H., Morii, N., Mishima, M., Narumiya, S., 1993. A rho-like protein is involved in the organization of the contractile ring in dividing sand dollar eggs. Zygote 1, 325–331.

McLaren, A., 1969. Can mouse blastocysts stimulate a uterine response before losing the zona pellucida? J. Reprod. Fertil. 19, 199–201.

Murphy, C., Grummt, M., Saffrich, R., Gournier, H., Rybin, V., Rubino, M., Auvinen, P., Parton, R.G., Zerial, M., 1996. Endosome dynamics regulated by a novel rho protein. Nature 384, 427–432.

Narumiya, S., 1996. The small GTPase Rho: cellular functions and signal transduction. J. Biochem. (Tokyo) 120, 215–228.

Nobes, C.D., Hall, A., 1999. Rho GTPases control polarity, protrusion, and adhesion during cell movement. J. Cell Biol. 144, 1235–1244.

Olson, M.F., Ashworth, A., Hall, A., 1995. An essential role for Rho, Rac, and Cdc42 GTPases in cell cycle progression through G1. Science 269, 1270–1272.

Ozil, J.P., Modlinski, J.A., 1986. Effects of electric field on fusion rate and survival of 2-cell rabbit embryos. J. Embryol. Exp. Morphol. 96, 211–228.

Rubin, E.J., Gill, D.M., Boquet, P., Popoff, M.R., 1988. Functional modification of a 21-kilodalton G protein when ADP-ribosylated by exoenzyme C3 of *Clostridium botulinum*. Mol. Cell. Biol. 8, 418–426.

Sakata, H., Rubin, J.S., Taylor, W.G., Miki, T., 2000. A rho-specific exchange factor ect2 is induced from S to M phases in regenerating mouse liver. Hepatology 32, 193–199.

Sambrook, J., Fritsch, E.F., Maniatis, T., 1989. Molecular Cloning: A Laboratory Manual, 2nd Edition. Cold Spring Harbor Laboratory, Cold Spring Harbor, NY.

Sugihara, K., Nakatsuji, N., Nakamura, K., Nakao, K., Hashimoto, R., Otani, H., Sakagami, H., Kondo, H., Nozawa, S., Aiba, A., Katsuki, M., 1998. Rac1 is required for the formation of three germ layers during gastrulation. Oncogene 17, 3427–3433.

Touré, A., Dorseuil, O., Morin, L., Timmons, P., Jegou, B., Reibel, L., Gacon, G., 1998. MgcRacGAP, a new human GTPase-activating protein for Rac and Cdc42 similar to *Drosophila* rotundRacGAP gene product, is expressed in male germ cells. J. Biol. Chem. 273, 6019–6023.

Van Aelst, L., D'Souza-Schorey, C., 1997. Rho GTPases and signalling networks. Genes Dev. 11, 2295–2322.

Verschueren, K., Remacle, J.E., Collart, C., Kraft, H., Baker, B.S., Tylzanowski, P., Nelles, L., Wuytens, G., Su, M.T., Bodmer, R., Smith, J.C., Huylebroeck, D., 1999. SIP1, a novel zinc Finger/Homeodomain repressor, interacts with smad proteins and binds to 5′-CACCT sequences in candidate target genes. J. Biol. Chem. 274, 20489–20498.

Volorio, S., Simon, G., Repetto, M., Cucciardi, M., Banfi, S., Borsani, G., Ballabio, A., Zollo, M., 1998. Sequencing analysis of forty-eight human image cDNA clones similar to *Drosophila* mutant protein. DNA Seq. 9, 307–315.

Voncken, J.W., van Schaick, H., Kaartinen, V., Deemer, K., Coates, T., Landing, B., Pattengale, P., Dorseuil, O., Bokoch, G.M., Groffen, J., Heisterkamp N., 1995. Increased neutrophil respiratory burst in bcr-null mutants. Cell 80, 719–728.

Wang, Z.J., Trounson, A., Dziadek, M., 1990. Developmental capacity of mechanically bisected mouse morulae and blastocysts. Reprod. Fertil. Dev. 2, 683–691.

Winkel, G.K., Nuccitelli, R., 1989. Octaploid mouse embryos produced by electrofusion polarize and cavitate at the same time as normal embryos. Gamete Res. 24, 93–107.

Wood, S.A., Allen, N.D., Rossant, J., Auerbach, A., Nagy, A., 1993. Non-injection methods for the production of embryonic stem cell–embryo chimeras. Nature 365, 87–89.

Wooltorton, E.J., Haliotis, T., Mueller, C.R., 1999. Identification and characterization of a transcript for a novel Rac GTPase-activating protein in terminally differentiating 3T3-L1 adipocytes. DNA Cell Biol. 18, 265–273.

Wurst, W., Joyner, A.L., 1993. Production of targeted embryonic stem cell clones. In: Joyner, A.L. (Ed.). Gene Targeting: A Practical Approach, IRL Press, Oxford, pp. 33–62.

Ziomek, C.A., Johnson, M.H., 1980. Cell surface interaction induces polarization of mouse 8-cell blastomeres at compaction. Cell 21, 935–942.

Zipkin, I.D., Kindt, R.M., Kenyon, C.J., 1997. Role of a new Rho family member in cell migration and axon guidance in *C. elegans*. Cell 90, 883–894.